

# Solubility Investigations in the Systems $\text{Li}_2\text{SO}_4 + \text{Li}_2\text{B}_4\text{O}_7 + \text{H}_2\text{O}$ and $\text{K}_2\text{SO}_4 + \text{K}_2\text{B}_4\text{O}_7 + \text{H}_2\text{O}$ at 288 K

Shi-hua Sang\* and Xiao Zhang

College of Materials and Chemistry & Chemical Engineering, Chengdu University of Technology, Chengdu 610059, P. R. China

The solubility, density, electrical conductivity, and pH of the ternary systems  $\text{Li}_2\text{SO}_4 + \text{Li}_2\text{B}_4\text{O}_7 + \text{H}_2\text{O}$  and  $\text{K}_2\text{SO}_4 + \text{K}_2\text{B}_4\text{O}_7 + \text{H}_2\text{O}$  at 288 K were determined experimentally by the isothermal solution saturation method. On the basis of the experimental results, the phase diagrams and property-composition diagrams were plotted. Phase equilibrium solids were  $\text{Li}_2\text{SO}_4 \cdot \text{H}_2\text{O}$  and  $\text{Li}_2\text{B}_4\text{O}_7 \cdot 3\text{H}_2\text{O}$  in the ternary  $\text{Li}_2\text{SO}_4 + \text{Li}_2\text{B}_4\text{O}_7 + \text{H}_2\text{O}$  system and  $\text{K}_2\text{SO}_4$  and  $\text{K}_2\text{B}_4\text{O}_7 \cdot 4\text{H}_2\text{O}$  in the ternary  $\text{K}_2\text{SO}_4 + \text{K}_2\text{B}_4\text{O}_7 + \text{H}_2\text{O}$  system at 288 K. The two ternary systems all belong to a simple cosaturated type, and the phase diagrams have one invariant point and two univariant curves. Double salts or solid solutions have not been found. The results for the ternary systems are discussed simply.

## 1. Introduction

There are many salt lakes on the Qinghai, Tibet plateau of China. A subtype of a sulfate salt lake brine is widely distributed in the area of the Qinghai, Tibet plateau, which has distinct characteristics from other brine types, and is famous for the high concentrations of lithium, potassium, and boron. The subtype of sulfate salt lake brines belong to the seven-compound system  $\text{Li}^+ - \text{K}^+ - \text{Na}^+ - \text{Mg}^{2+} - \text{Cl}^- - \text{SO}_4^{2-} - \text{B}_4\text{O}_7^{2-} - \text{H}_2\text{O}$ .<sup>1</sup>

Salt lake brines of high concentration contain abundant mineral resources. To exploit the resources of this subtype of sulfate salt lake brine system, solid–liquid equilibrium studies of the brines at different temperatures are necessary.<sup>2</sup>

Some solid–liquid phase equilibrium systems of the sulfate salt lake brine have been studied at 298 K: the quinary system  $\text{Li}^+, \text{Mg}^{2+}/\text{Cl}^-, \text{SO}_4^{2-}, \text{B}_4\text{O}_7^{2-} - \text{H}_2\text{O}$ ;<sup>3</sup> the quaternary systems  $\text{Li}^+, \text{Mg}^{2+}/\text{SO}_4^{2-}, \text{B}_4\text{O}_7^{2-} - \text{H}_2\text{O}$ ;<sup>4</sup> and  $\text{MgSO}_4 - \text{MgB}_4\text{O}_7 - \text{MgCl}_2 - \text{H}_2\text{O}$ ;<sup>5</sup> and the ternary system  $\text{MgSO}_4 - \text{MgB}_4\text{O}_7 - \text{H}_2\text{O}$ .<sup>6</sup> Furthermore, ternary systems including borates have also been reported at  $T = 288 \text{ K}$ :  $\text{Li}_2\text{B}_4\text{O}_7 + \text{Na}_2\text{B}_4\text{O}_7 + \text{H}_2\text{O}$ ;<sup>7</sup>  $\text{K}_2\text{B}_4\text{O}_7 + \text{Li}_2\text{B}_4\text{O}_7 + \text{H}_2\text{O}$ ;<sup>7</sup> and  $\text{K}_2\text{B}_4\text{O}_7 + \text{Na}_2\text{B}_4\text{O}_7 + \text{H}_2\text{O}$ .<sup>8</sup> The ternary systems are subsystems of the sulfate salt lake brine, which are the bases of quaternary and quinary phase equilibrium for the brines. The phase equilibria of the ternary system  $\text{Li}_2\text{SO}_4 + \text{Li}_2\text{B}_4\text{O}_7 + \text{H}_2\text{O}$  at 298 K have been reported.<sup>9</sup> However, the experimental studies of equilibrium in the systems  $\text{Li}_2\text{SO}_4 + \text{Li}_2\text{B}_4\text{O}_7 + \text{H}_2\text{O}$  and  $\text{K}_2\text{SO}_4 + \text{K}_2\text{B}_4\text{O}_7 + \text{H}_2\text{O}$  at 288 K have not been reported. In this paper, the phase equilibria and densities of the equilibrated solution for the ternary systems listed above are reported because the average temperature of the Qinghai, Tibet plateau in summer is about 288 K.

## 2. Experimental Section

**2.1. Instruments and Reagents.** All reactants used in this study were of analytical purity grade and obtained from the following suppliers:  $\text{Li}_2\text{SO}_4 \cdot \text{H}_2\text{O}$ , purity of 99.5 %,  $\text{K}_2\text{SO}_4$ , purity of 99.5 % (ChengDu KeLun Chemical Reagent

Factory, China),  $\text{Li}_2\text{B}_4\text{O}_7$ , 99.8 %, and  $\text{K}_2\text{B}_4\text{O}_7 \cdot 4\text{H}_2\text{O}$  purity of 99.5 % (BeiJing XingHua Chemical Reagent Factory, China). The water used was bidistilled.

A HZS-H type thermostatted vibrator with a precision of  $\pm 0.1 \text{ K}$  was used for the equilibrium measurements. A PHS-3C digital acidometer (precision:  $\pm 0.01$ ) was used for the measurement of the pH of the equilibrated solutions. A DDZ-11A type conductometer (precision:  $\pm 0.01 \text{ mS} \cdot \text{cm}^{-1}$ ) was used for the measurement of the electrical conductivity of the equilibrated solutions.

**2.2. Experimental Method.** The experiments for phase equilibria have been done by the method of isothermal solution saturation. The system points for the ternary system were obtained by adding the second component gradually on the basis of the single salt saturation points at 288 K. The respective mixtures were placed in bottles of 100 mL for the solubility experiments and the bottles placed in the thermostatted vibrator (HZS-H). The bottles with solution were stirred for one week to promote the establishment of equilibrium. The time to reach equilibrium was about three to six days. The solutions were taken out periodically for chemical analysis. When the components of the solution did not change, equilibrium was established. After equilibrium, the compositions of solution were determined by methods of chemical analysis.

The pH values and electrical conductivity values of the equilibrated solutions were measured. The densities of the solution were measured by a pycnometer with an uncertainty of  $0.0002 \text{ g} \cdot \text{cm}^{-3}$ .

**2.3. Identification of Solid Phase.** After the equilibration finished, the solids were separated from the solutions. Then, the wet residue mixture was filtered; wet crystals were separated from each other according to crystal shapes as well as possible. The wet residual solids were evaluated by chemical analysis. The solids were also determined approximately by the Schreinemaker wet residue method, and further identification was done by X-ray diffraction.

**2.4. Analytical Methods.**<sup>10</sup> The potassium ion concentration was measured by a sodium tetraphenylborate–hexadecyl trimethyl ammonium bromide titration (precision:  $\pm 0.5 \%$ ).

\* Corresponding author. E-mail: sangsh@cdu.edu.cn and sangshihua@sina.com.

**Table 1.** Solubility, Density  $\rho$ , and Electrical Conductivity  $\kappa$  of Solutions in the Ternary System  $\text{Li}_2\text{SO}_4$  (1) +  $\text{Li}_2\text{B}_4\text{O}_7$  (2) +  $\text{H}_2\text{O}$  (3) at 288 K

NO	composition of solution 100 $w_b$			properties of solution			
	100 $w_1$	100 $w_2$	100 $w_3$	density $\rho/(\text{g}\cdot\text{cm}^{-3})$	elect. cond. $\kappa/(\text{mS}\cdot\text{cm}^{-1})$	pH	equilibrium solid phase
1 (A)	0.00	2.55	97.45	1.0193	7.51	9.62	$\text{Li}_2\text{B}_4\text{O}_7\cdot 3\text{H}_2\text{O}$
2	3.48	2.13	94.39	1.0509	10.64	9.60	$\text{Li}_2\text{B}_4\text{O}_7\cdot 3\text{H}_2\text{O}$
3	5.09	1.88	93.03	1.0786	10.75	9.45	$\text{Li}_2\text{B}_4\text{O}_7\cdot 3\text{H}_2\text{O}$
4	10.00	1.72	88.28	1.0969	11.63	9.31	$\text{Li}_2\text{B}_4\text{O}_7\cdot 3\text{H}_2\text{O}$
5	14.39	1.32	84.29	1.1276	11.74	9.21	$\text{Li}_2\text{B}_4\text{O}_7\cdot 3\text{H}_2\text{O}$
6	18.04	1.30	80.66	1.1549	11.63	9.12	$\text{Li}_2\text{B}_4\text{O}_7\cdot 3\text{H}_2\text{O}$
7	21.03	1.05	77.92	1.1735	10.62	9.00	$\text{Li}_2\text{B}_4\text{O}_7\cdot 3\text{H}_2\text{O}$
8 (E)	24.50	0.88	74.62	1.2126	10.53	8.80	$\text{Li}_2\text{B}_4\text{O}_7\cdot 3\text{H}_2\text{O}$ + $\text{Li}_2\text{SO}_4\cdot\text{H}_2\text{O}$
9	23.60	0.68	75.72	1.2067	11.41	8.77	$\text{Li}_2\text{SO}_4\cdot\text{H}_2\text{O}$
10	23.51	0.50	75.99	1.2054	11.41	8.78	$\text{Li}_2\text{SO}_4\cdot\text{H}_2\text{O}$
11	24.85	0.35	74.80	1.2140	10.08	8.83	$\text{Li}_2\text{SO}_4\cdot\text{H}_2\text{O}$
12 (B)	25.92	0.00	74.08	1.2092	9.20	8.30	$\text{Li}_2\text{SO}_4\cdot\text{H}_2\text{O}$

The borate ion concentration was evaluated by basic titration with mannitol (precision:  $\pm 0.3\%$ ). The lithium ion concentration was determined by atomic absorption spectrophotometry (AAS); the relative error of the determination of the lithium ion was estimated to be less than 1%. The sulfate ion concentration ( $\text{SO}_4^{2-}$ ) was determined by a method of mixing barium chloride and magnesium chloride–EDTA (ethylenediaminetetraacetic acid) titration (uncertainty of 0.5%).

### 3. Results and Discussion

**3.1.  $\text{Li}_2\text{SO}_4$  +  $\text{Li}_2\text{B}_4\text{O}_7$  +  $\text{H}_2\text{O}$  System.** The experimental results of solubilities and densities for the ternary system  $\text{Li}_2\text{SO}_4$  +  $\text{Li}_2\text{B}_4\text{O}_7$  +  $\text{H}_2\text{O}$  at 288 K were determined and are tabulated in Table 1. The respective ion concentration values are expressed in mass fraction  $w_b$ . The solution density ( $\rho$ ) is given in grams per centimeter, electrical conductivity ( $\kappa$ ) is given in milli-Siemens per centimeter. The corresponding phase diagram is plotted in Figure 1. Figure 2 is an enlarged part of the phase diagram of Figure 1.

In Figure 1, point A and point B represent the solubility of the binary systems of  $\text{Li}_2\text{B}_4\text{O}_7$ – $\text{H}_2\text{O}$  and  $\text{Li}_2\text{SO}_4$ – $\text{H}_2\text{O}$  at

288 K with a mass fraction (100  $w_b$ ) of 2.55 and 25.92, respectively. Point L and point S in Figure 1 represent the solid phase  $\text{Li}_2\text{B}_4\text{O}_7\cdot 3\text{H}_2\text{O}$  and  $\text{Li}_2\text{SO}_4\cdot\text{H}_2\text{O}$ , respectively. In the phase diagram of the ternary system  $\text{Li}_2\text{SO}_4$  +  $\text{Li}_2\text{B}_4\text{O}_7$  +  $\text{H}_2\text{O}$  at 288 K, there are two single salt crystallization zones of  $\text{Li}_2\text{SO}_4\cdot\text{H}_2\text{O}$  and  $\text{Li}_2\text{B}_4\text{O}_7\cdot 3\text{H}_2\text{O}$ , one invariant point E, and two univariant curves AE and BE. The crystallization area  $\text{Li}_2\text{B}_4\text{O}_7\cdot 3\text{H}_2\text{O}$  (AEL) in the phase diagram is bigger than that of  $\text{Li}_2\text{SO}_4\cdot\text{H}_2\text{O}$  (BES). The lithium borate concentration with increasing concentration of lithium sulfate (AE curve) diminishes toward the invariant point (E). The monotonic curves imply that no chemical compound is formed in the studied ternary system.

On the basis of data collected in Table 1, relationships between the solution properties (density, pH, electrical conductivity) and the salt concentration values expressed in mass fractions (Figure 3) are found. The physicochemical properties of the experimental data and Figure 3 show that the equilibrium solution density values in the ternary system  $\text{Li}_2\text{SO}_4$  +  $\text{Li}_2\text{B}_4\text{O}_7$  +  $\text{H}_2\text{O}$  at 288 K increased with a rise of lithium sulfate concentration, reaching a maximum value at invariant point E (Figure 3a). Electrical conductivity values, however, increased at first and then fell with the rise of ion concentration (Figure

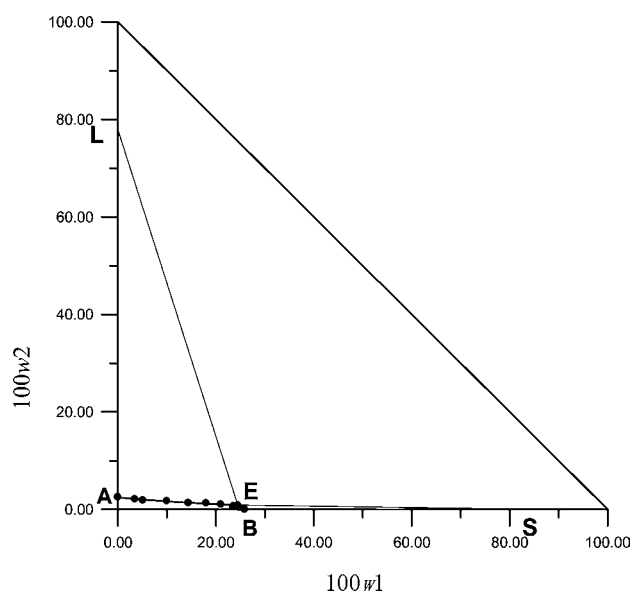


**Figure 1.** Phase diagram of the ternary system  $\text{Li}_2\text{SO}_4$  (1) +  $\text{Li}_2\text{B}_4\text{O}_7$  (2) +  $\text{H}_2\text{O}$  (3) at 288 K. ●, experimental data points; A, binary system  $\text{Li}_2\text{B}_4\text{O}_7$ – $\text{H}_2\text{O}$  saturation point; B, binary system  $\text{Li}_2\text{SO}_4$ – $\text{H}_2\text{O}$  saturation point; L, solid phase point ( $\text{Li}_2\text{B}_4\text{O}_7\cdot 3\text{H}_2\text{O}$ ); S, solid phase point ( $\text{Li}_2\text{SO}_4\cdot\text{H}_2\text{O}$ ); E, invariant point saturated with  $\text{Li}_2\text{B}_4\text{O}_7\cdot 3\text{H}_2\text{O}$  and  $\text{Li}_2\text{SO}_4\cdot\text{H}_2\text{O}$ .

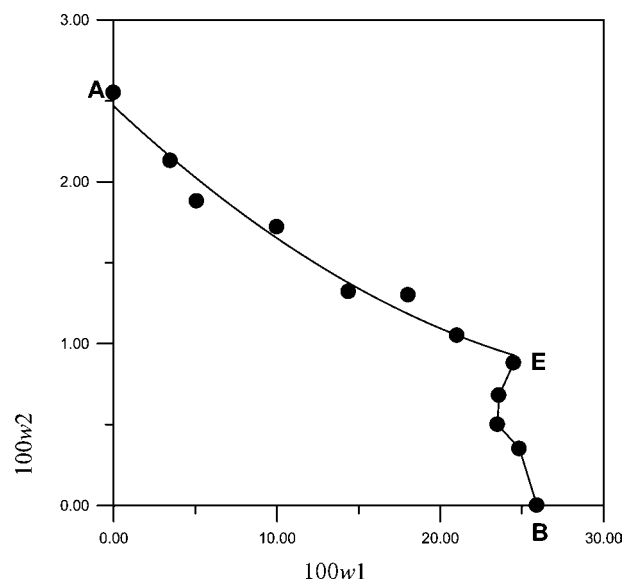


**Figure 2.** Enlarged part of the phase diagram of the ternary system  $\text{Li}_2\text{SO}_4$  (1) +  $\text{Li}_2\text{B}_4\text{O}_7$  (2) +  $\text{H}_2\text{O}$  (3) at 288 K. ●, experimental data points; A, binary system  $\text{Li}_2\text{B}_4\text{O}_7$ – $\text{H}_2\text{O}$  saturation point; B, binary system  $\text{Li}_2\text{SO}_4$ – $\text{H}_2\text{O}$  saturation point; E, invariant point saturated with  $\text{Li}_2\text{B}_4\text{O}_7\cdot 3\text{H}_2\text{O}$  and  $\text{Li}_2\text{SO}_4\cdot\text{H}_2\text{O}$ .

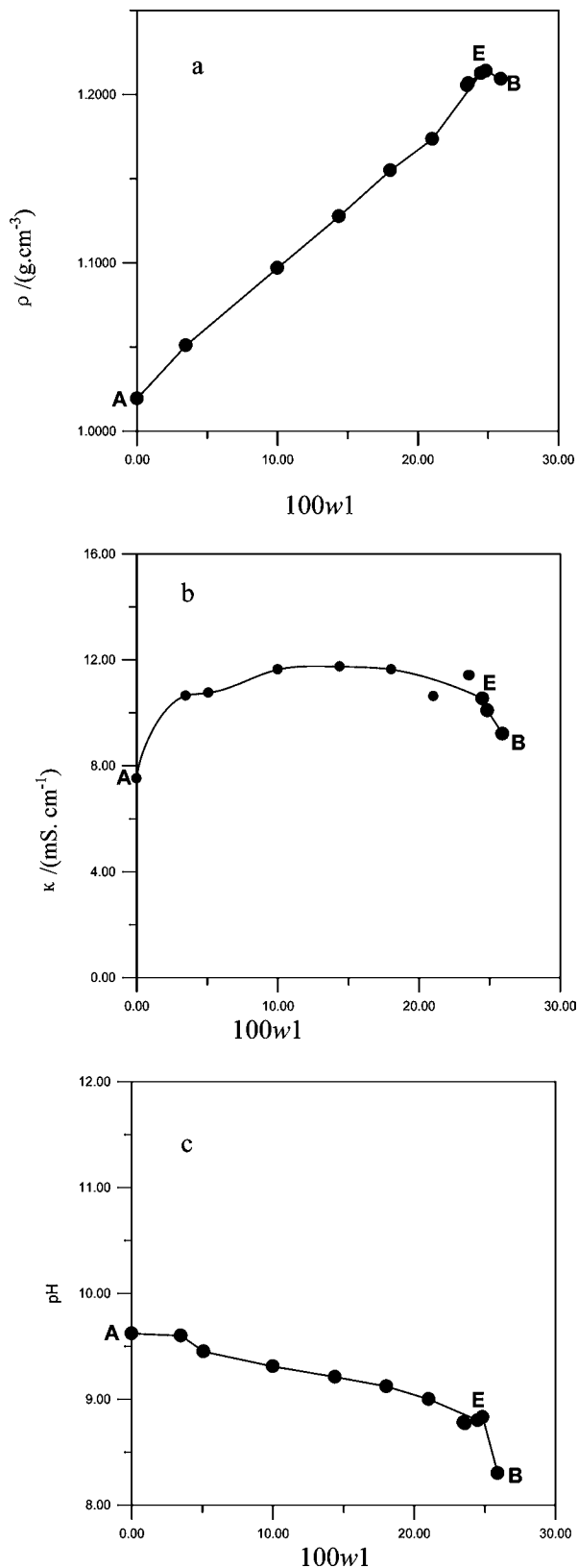


**Figure 3.** Physicochemical property composition diagrams for the ternary system  $\text{Li}_2\text{SO}_4$  (1) +  $\text{Li}_2\text{B}_4\text{O}_7$  (2) +  $\text{H}_2\text{O}$  (3) at 288 K for (a) density, (b) electrical conductivity, and (c) pH. ●, experimental data points; AE, physicochemical property values (density, electrical conductivity, and pH) corresponding to univariant curves AE; BE, physicochemical property values (density, electrical conductivity, and pH) corresponding to univariant curves BE; E, physicochemical property values corresponding to invariant point E.

3b). The pH values fell with a rise of ion concentration on the whole (Figure 3c).

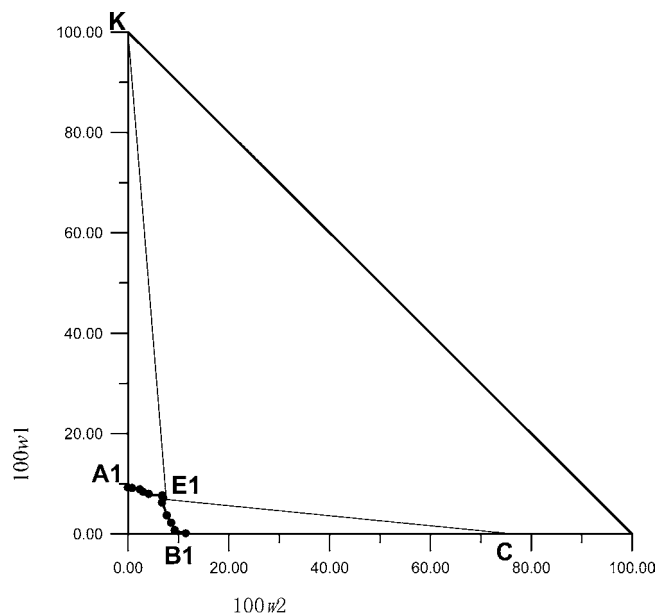


**Figure 4.** Phase diagram of the ternary system  $\text{K}_2\text{SO}_4$  (1)– $\text{K}_2\text{B}_4\text{O}_7$  (2)– $\text{H}_2\text{O}$  (3) at 288 K. ●, experimental data points; A1, binary system  $\text{K}_2\text{SO}_4$ – $\text{H}_2\text{O}$  saturation point; B1, binary system  $\text{K}_2\text{B}_4\text{O}_7$ – $\text{H}_2\text{O}$  saturation point; K, solid phase point ( $\text{K}_2\text{SO}_4$ ); C, solid phase point ( $\text{K}_2\text{B}_4\text{O}_7 \cdot 4\text{H}_2\text{O}$ ); E1, invariant point saturated with  $\text{K}_2\text{SO}_4$  and  $\text{K}_2\text{B}_4\text{O}_7 \cdot 4\text{H}_2\text{O}$ .

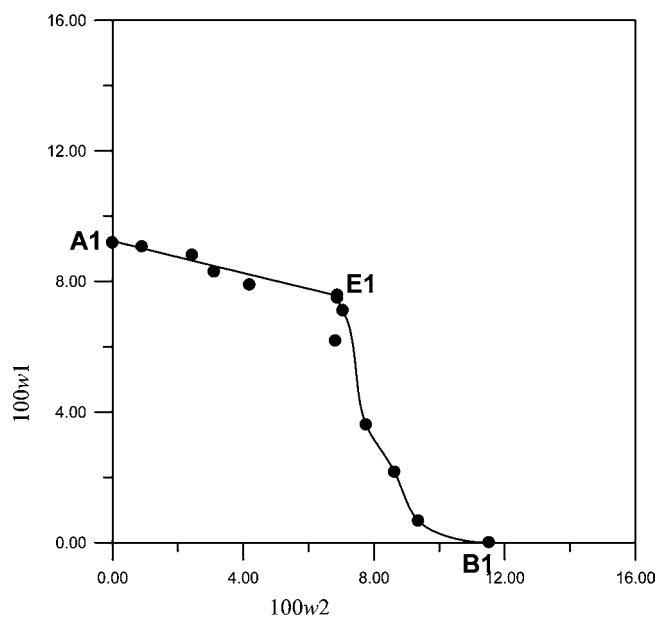


**Figure 5.** Enlarged part of the phase diagram of the ternary system  $\text{K}_2\text{SO}_4$  (1)– $\text{K}_2\text{B}_4\text{O}_7$  (2)– $\text{H}_2\text{O}$  (3) at 288 K. ●, experimental data points; A1, binary system  $\text{K}_2\text{SO}_4$ – $\text{H}_2\text{O}$  saturation point; B1, binary system  $\text{K}_2\text{B}_4\text{O}_7$ – $\text{H}_2\text{O}$  saturation point; E1, invariant point saturated with  $\text{K}_2\text{SO}_4$  and  $\text{K}_2\text{B}_4\text{O}_7 \cdot 4\text{H}_2\text{O}$ .

**3.2.  $\text{K}_2\text{SO}_4 + \text{K}_2\text{B}_4\text{O}_7 + \text{H}_2\text{O}$  System.** The experimental results of solubilities and properties for the ternary system  $\text{K}_2\text{SO}_4 + \text{K}_2\text{B}_4\text{O}_7 + \text{H}_2\text{O}$  at 288 K are presented in Table 2, and the corresponding phase diagrams are shown in Figures 4 and 5. Figure 5 is an enlarged part of the phase diagram shown in Figure 4.

In Figure 4, points A1 and B1 represent the solubility of the binary systems of  $\text{K}_2\text{SO}_4$ – $\text{H}_2\text{O}$  and  $\text{K}_2\text{B}_4\text{O}_7$ – $\text{H}_2\text{O}$  at 288 K with a mass fraction ( $100 w_b$ ) of 9.28 and 11.52, respectively. The

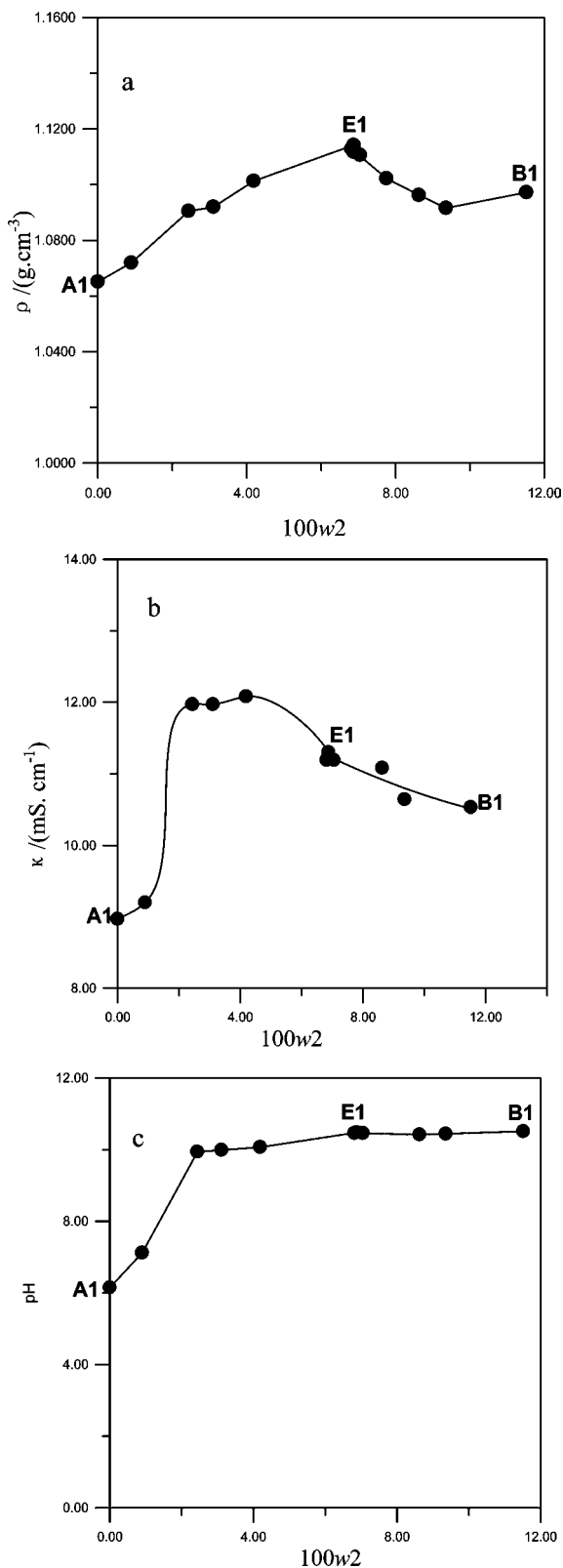


**Figure 6.** Physicochemical property composition diagrams for the ternary system  $\text{K}_2\text{SO}_4$  (1) +  $\text{K}_2\text{B}_4\text{O}_7$  (2) +  $\text{H}_2\text{O}$  (3) at 288 K for (a) density, (b) electrical conductivity, and (c) pH. ●, experimental data points; A1E1, physicochemical property values (density, electrical conductivity, and pH) corresponding to univariant curves A1E1; B1E1, physicochemical property values (density, electrical conductivity, and pH) corresponding to univariant curves B1E1; E1, physicochemical property values corresponding to invariant point E1.

points K and C in Figure 4 represent the solid phases  $\text{K}_2\text{SO}_4$  and  $\text{K}_2\text{B}_4\text{O}_7 \cdot 4\text{H}_2\text{O}$ , respectively.

**Table 2.** Solubility, Density  $\rho$ , and Electrical Conductivity  $\kappa$  of Solutions in the Ternary System  $\text{K}_2\text{SO}_4$  (1) +  $\text{K}_2\text{B}_4\text{O}_7$  (2) +  $\text{H}_2\text{O}$  (3) at 288 K

NO	composition of solution 100 $w_b$			properties of solution		
	100 $w_1$	100 $w_2$	100 $w_3$	$\rho$ ( $\text{g}\cdot\text{cm}^{-3}$ )	$\kappa$ ( $\text{mS}\cdot\text{cm}^{-1}$ )	pH
1 (A1)	9.28	0.00	90.72	1.0651	8.97	6.15 $\text{K}_2\text{SO}_4$
2	9.06	0.90	90.04	1.0719	9.20	7.12 $\text{K}_2\text{SO}_4$
3	8.80	2.44	88.76	1.0905	11.97	9.94 $\text{K}_2\text{SO}_4$
4	8.29	3.11	88.60	1.0920	11.97	9.99 $\text{K}_2\text{SO}_4$
5	7.89	4.19	87.92	1.1013	12.08	10.07 $\text{K}_2\text{SO}_4$
6 (E1)	7.57	6.88	85.55	1.1142	11.30	10.48 $\text{K}_2\text{B}_4\text{O}_7 \cdot 4\text{H}_2\text{O}$ + $\text{K}_2\text{SO}_4$
7	7.49	6.88	85.63	1.1117	11.19	10.46 $\text{K}_2\text{B}_4\text{O}_7 \cdot 4\text{H}_2\text{O}$
8	7.10	7.05	85.85	1.1106	11.19	10.46 $\text{K}_2\text{B}_4\text{O}_7 \cdot 4\text{H}_2\text{O}$
9	6.18	6.82	87.00	1.1128	10.19	10.49 $\text{K}_2\text{B}_4\text{O}_7 \cdot 4\text{H}_2\text{O}$
10	3.61	7.76	88.63	1.1022	11.08	10.42 $\text{K}_2\text{B}_4\text{O}_7 \cdot 4\text{H}_2\text{O}$
11	2.16	8.63	89.21	1.0962	10.64	10.44 $\text{K}_2\text{B}_4\text{O}_7 \cdot 4\text{H}_2\text{O}$
12	0.66	9.36	89.98	1.0916	9.42	10.44 $\text{K}_2\text{B}_4\text{O}_7 \cdot 4\text{H}_2\text{O}$
13 (B1)	0.00	11.52	88.48	1.0868	10.53	10.51 $\text{K}_2\text{B}_4\text{O}_7 \cdot 4\text{H}_2\text{O}$

In Figure 4, there are two crystallization zones,  $\text{K}_2\text{SO}_4$  (A1E1K) and  $\text{K}_2\text{B}_4\text{O}_7 \cdot 4\text{H}_2\text{O}$  (B1E1C), one isothermal invariant point E1, and two univariant curves A1E1 and B1E1. The A1E1 curve corresponds to the solubility isotherms where the solution was saturated with  $\text{K}_2\text{SO}_4$ . The B1E1 curve corresponds to the solubility isotherms where the solution was saturated with  $\text{K}_2\text{B}_4\text{O}_7 \cdot 4\text{H}_2\text{O}$ . The invariant point E1 corresponds to the solution saturated with the salts  $\text{K}_2\text{SO}_4$  and  $\text{K}_2\text{B}_4\text{O}_7 \cdot 4\text{H}_2\text{O}$ .

The physicochemical property composition diagrams are given in Figure 6 on the basis of the experimental data in Table 2. The densities of the experimental data and Figure 6a show that the equilibrium solution density values increase with a rise of the potassium borate concentration in the A1E1 curve, reaching a maximum value at invariant point E1 (Figure 6a); however, the density decreases in the B1E1 curve with a rise of the potassium borate concentration and reaches the point (B1) of solutions saturated  $\text{K}_2\text{B}_4\text{O}_7 \cdot 4\text{H}_2\text{O}$ . It can be found that the electrical conductivity increases at first and then falls with a rise of ion concentration (Figure 6b). The pH values increase slightly on the whole (Figure 6c).

#### 4. Conclusion

The solubilities and the densities of solution in the systems  $\text{Li}_2\text{SO}_4 + \text{Li}_2\text{B}_4\text{O}_7 + \text{H}_2\text{O}$  and  $\text{K}_2\text{SO}_4 + \text{K}_2\text{B}_4\text{O}_7 + \text{H}_2\text{O}$  at 288 K were determined experimentally. According to the experimental data measured, the phase diagrams and density-composition diagrams were constructed. The equilibrium solid phases for the system  $\text{Li}_2\text{SO}_4 + \text{Li}_2\text{B}_4\text{O}_7 + \text{H}_2\text{O}$  at 288 K are  $\text{Li}_2\text{SO}_4 \cdot \text{H}_2\text{O}$  and  $\text{Li}_2\text{B}_4\text{O}_7 \cdot 3\text{H}_2\text{O}$ . The equilibrium solid phases for the system  $\text{K}_2\text{SO}_4 + \text{K}_2\text{B}_4\text{O}_7 + \text{H}_2\text{O}$  at 288 K are  $\text{K}_2\text{SO}_4$  and  $\text{K}_2\text{B}_4\text{O}_7 \cdot 4\text{H}_2\text{O}$ . Simple discussions were made on the construction of the diagram.

#### Literature Cited

- (1) Zheng, M. P.; Xiang, J. *Salt Lakes of Qinghai-Xizang (Tibet) Plateau* (in Chinese); Science and Technology Press: Beijing, 1989.
- (2) Song, P. S. Comprehensive Utilization of Salt Lake Resources. *J. Salt Lake Res.* **1993**, *1*, 68–80.
- (3) Sun, B.; Song, P. S.; Du, X. H. A Study on Solution and Phase Transformation of Some Magnesium Borates. *J. Salt Lake Res.* **1994**, *2*, 26–29.
- (4) Song, P. S.; Fu, H. A. Solubilities and Properties of Solution in the Reciprocal System  $\text{Li}^+$ ,  $\text{Mg}^{2+}/\text{B}_4\text{O}_7^{2-}$ ,  $\text{SO}_4^{2-}$ -  $\text{H}_2\text{O}$  at 25°C. *J. Inorg. Chem.* **1991**, *7*, 344–347.

- (5) Du, X. H.; Song, P. S.; Zhang, J. T. Phase Equilibrium in the Quaternary System  $\text{MgB}_4\text{O}_7$  -  $\text{MgSO}_4$ -  $\text{MgCl}_2$  -  $\text{H}_2\text{O}$  at 25°C. *J. Wuhan Inst. Chem. Technol.* **2000**, *22*, 13–16.
- (6) Song, P. S.; Du, X. H.; Sun, B. Study on The Ternary System  $\text{MgB}_4\text{O}_7$  -  $\text{MgSO}_4$  -  $\text{H}_2\text{O}$  at 25°C. *Chin. Sci. Bull.* **1988**, *33*, 1971–1973.
- (7) Sang, S. H.; Yin, H. A.; Tang, M. L. Solubility Investigations in the Systems  $\text{K}_2\text{B}_4\text{O}_7$  +  $\text{Li}_2\text{B}_4\text{O}_7$  +  $\text{H}_2\text{O}$  and  $\text{Na}_2\text{B}_4\text{O}_7$  +  $\text{Li}_2\text{B}_4\text{O}_7$  +  $\text{H}_2\text{O}$  at  $T = 288$  K. *J. Chem. Eng. Data* **2004**, *49*, 1586–1589.
- (8) Sang, S. H.; Tang, M. L.; Yin, H. A.; Zhang, Y. X. A Study on Phase Equilibria for the Ternary System  $\text{K}_2\text{B}_4\text{O}_7$ - $\text{Na}_2\text{B}_4\text{O}_7$ - $\text{H}_2\text{O}$  at 288K. *J. Sea-Lake Chem. Ind.* **2002**, *31*, 16–18.
- (9) Song, P. S.; Du, X. H.; Xu, H. C. The phase equilibrium and properties of the saturated solution in the ternary system  $\text{Li}_2\text{B}_4\text{O}_7$  -  $\text{Li}_2\text{SO}_4$  -  $\text{H}_2\text{O}$  at 25°C. *Chin. Sci. Bull.* **1984**, *29* (8), 1072–1076.
- (10) *Institute of Qinghai Salt-Lake, Chinese Academy of Science, Analytical Methods of Brines and Salts* (in Chinese); Science Press: Beijing, 1988.

Received for review June 3, 2009. Accepted November 27, 2009. The project was supported by the New Century Excellent Talents in the University of China (NCET-07-0125), the National Nature Science Foundation of China (No. 40973047), and the Young Science Foundation of Sichuan Province in China (08ZQ026-017).

JE900474S